

# Factors affecting the characteristics of the negative electrodes for nickel-metal hydride batteries

Jin Hongmei<sup>a,\*</sup>, Li Guoxun<sup>b</sup>, Zhou Chuanhua<sup>b</sup>, Wang Ruikun<sup>b</sup>

<sup>a</sup> Department of Materials Science, National University of Singapore, Singapore 119260

<sup>b</sup> General Research Institute for Non-ferrous Metal, Beijing 100088, China

Received 8 October 1998; accepted 24 October 1998

## Abstract

The effects of annealing, pulverization process and particle size on the electrode performance were examined. Annealing flattened the p–c isotherm and improved the cycle life, but decreased the maximum hydrogen absorption content of the alloy and therefore decreased the discharge capacity of the electrode. The initial discharge capacity and maximum discharge capacity of the electrode are higher by using the hydrogen desorption pulverization method. The results of different particle sizes on the characteristics of the electrodes indicated that particles between 200–300 mesh and below 500 mesh has good performance. This may be related to the charge-transfer resistance, contact resistance and other factors which determine the cycle life degradation. © 1999 Elsevier Science S.A. All rights reserved.

**Keywords:** Annealing; Particle size; Pulverization method; Electrochemical properties

## 1. Introduction

Nickel-metal hydride batteries employing hydrogen storage alloys as a negative electrode material have several inherent advantages over conventional nickel–cadmium batteries with respect to storage capacity, ‘cleanness,’ and tolerance to overcharge and overdischarge [1–3]. In recent years, extensive research and development of rechargeable batteries of this type have been carried out directed practical use [4–8]. In general, the characteristics of the negative electrode are affected by alloy preparation. In this work,  $\text{La}_{0.9}\text{Nd}_{0.1}\text{Ni}_{3.55}\text{Co}_{0.75}\text{Mn}_{0.4}\text{Al}_{0.3}$  alloy was employed as the negative electrode material. The effects of annealing, pulverization method and particle sizes on the charge–discharge performance were investigated.

## 2. Experimental

The  $\text{La}_{0.9}\text{Nd}_{0.1}\text{Ni}_{3.55}\text{Co}_{0.75}\text{Mn}_{0.4}\text{Al}_{0.3}$  material was prepared as a button by mixing the appropriate amounts of

metals, which had a purity of higher than 99.9 wt.%, and melted under purified Ar. The button was remelted several times to ensure homogeneity. Part of as-produced alloy was vacuum annealed in an electric furnace for 48 h at a temperature of  $T = 1150\text{--}1200^\circ\text{C}$  to examine the annealing effect. X-ray diffraction analysis was used to determine the crystal structure. JSM-6400 scanning electron microscope with energy dispersive analyzer of X-ray was used to investigate the microstructure and the elements distribution in the alloy. The pressure composition isotherm (p–c–t curves) was measured using a home-built p–c–t curve[9] surveying instrument.

For the electrochemical properties, the as-produced alloy was ground into powder either by the mechanical method or by a hydrogen desorption process. The pulverized powder was separated into three particle sizes of 200–300 mesh, 300–500 mesh and below 500 mesh by passing through sieves after the hydrogen desorption pulverization. To determine the discharge capacity, the alloy powder was mixed with fine Cu powder in a weight ratio of 1:4. The mixture was pressed into disks with weight of 1 g, 13 mm in diameter and 1.1 mm in thickness at a pressure of  $3 \times 10^7 \text{ N m}^{-2}$ . Before the determination, the sample was immersed in 6 N KOH electrolyte at least 12 h. NiOOH and Hg/HgO were used as the counter elec-

\* Corresponding author. Institute of High Performance Computing, 89B Science Park drive, 01-05/08, Singapore 118261, Singapore. Tel.: +65-7709277; Fax: +65-7780522; E-mail: jinhm@ihpc.nus.edu.sg

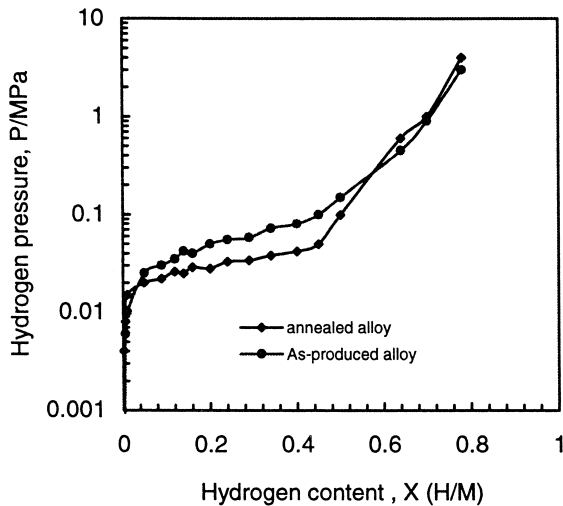


Fig. 1. Desorption  $p$ - $c$  isotherm for as-produced and annealed alloys.

trode and reference electrode, respectively. The negative electrode was charged for 2 h at  $200 \text{ mA g}^{-1}$  and discharged to  $-0.65 \text{ V}$  at  $100 \text{ mA g}^{-1}$  vs. Hg/HgO electrode. For cycle life, the electrode was prepared by mixing 200–300 mesh alloy (obtained by the hydrogen desorption method) with appropriate PVA and PTFE. The mixture was then pressed onto a  $2 \times 2$ -cm nickel mesh screen attached to a nickel wire connection which was then sandwiched between two positive NiOOH electrodes. After immersion in KOH electrolyte for more than 12 h, the electrode was charged for 2.33 h at  $150 \text{ mA}^{-1}$  and discharged at a current of  $150 \text{ mA/g}$  to  $-0.9 \text{ V}$ .

### 3. Results and discussion

#### 3.1. The effect of annealing

Desorption  $p$ - $c$  isotherms at  $30^\circ\text{C}$  of as-produced and the alloy annealed at  $1150$ – $1200^\circ\text{C}$  are shown in Fig. 1. Annealing flattened the plateau slope but decreased the maximum hydrogen content. This indicated that the microstrain which was introduced during solidification has been released after annealing. The composition of the alloy and the crystal lattice became homogeneous. However due to the decrease of maximum hydrogen content, the discharge capacity of alloy may have been decreased.

Table 1 lists the composition of the grain and grain boundary for as-produced and annealed alloys. For as-produced alloy, the content (at.%) of elements like Co, Mn, Al were higher at the grain boundaries. But the content of rare earth and nickel are higher within the grain. This suggests that, for as-produced alloy, Co, Mn, and Al are mainly concentrated at the grain boundary, and rare earth are mostly distributed within the grain. After annealing, the concentration of Co, Al at the grain boundaries are further increased and element La in the grain is also

Table 1

Composition analysis results in the grain and grain boundary before and after annealing

	La	Nd	Ni	Co	Mn	Al
M	27.91	4.81	54.19	10.8	1.48	0.91
M <sub>annealing</sub>	29.73	3.27	52.99	9.88	2.58	1.59
G	3.34	0.21	52.02	22.12	18.7	3.82
G <sub>annealing</sub>	1.03	0.28	54.83	26.64	12.88	4.34

M—In the grain.

G—Grain boundary.

further increased. However, the concentration of Mn at the grain boundary is significantly decreased. This shows that annealing distributes the Mn. The diffusion of Mn may have caused a relatively homogeneous composition in the dominate phase, therefore both the plateau slope and pressure of the  $p$ - $c$  isotherm were decreased by annealing.

Fig. 2 shows the cycle life of as-produced alloy and alloys annealed for 48 h. From Fig. 2 we can see that annealing decreased the discharge capacity but increased the cycle life. This result is in agreement with the  $p$ - $c$  isotherm. According to Ref. [10], there are two important factors which determine the degradation of the cycle life. These two factors are discrete lattice expansion upon phase transition during hydride formation and the mechanical properties of the hydride-forming alloys. The lattice expansion is directly related to the hydrogen content in the unit cell. Because the annealing decreased the maximum hydrogen content, it inevitably will reduce the lattice expansion of the alloy. Therefore, the degradation of cycle life due to the lattice expansion will be decreased, and the cycle life of the electrode should be improved.

Other research workers [11] indicated that a wider plateau region in  $p$ - $c$  isotherm can bring a larger discrete lattice expansion and promote the degradation of cycle life.

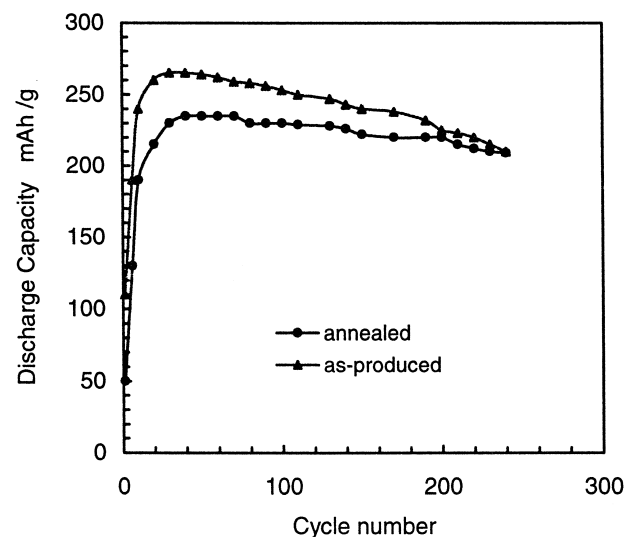


Fig. 2. Discharge capacity vs. the number of cycles for annealed and as-produced alloy.

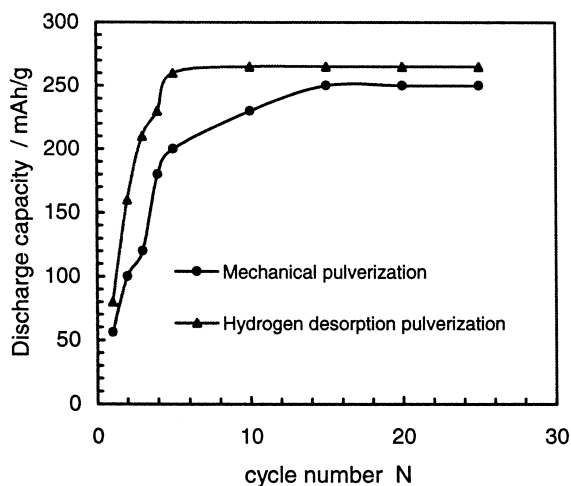


Fig. 3. Effect of pulverization process on discharge capacity.

So materials should be developed which have the plateau region narrow enough to limit the discrete lattice expansion.

### 3.2. Effect of pulverization method

The discharge capacity of the electrode after the two different pulverization methods are shown in Fig. 3. According to Fig. 3, the discharge capacity of electrode is higher and the alloy is easier to activate using the hydrogen desorption pulverization method. Fig. 4 shows SEM images of the powder from two different pulverization methods. It can be seen that the particles are more uniform after hydrogen desorption pulverization than after mechanical pulverization. In addition, small cracks can also be found in the interior of the particles after hydrogen desorption pulverization. These small cracks may have contributed to the increase of the fresh surfaces of alloy, and they may have promoted the kinetics of activation process.

### 3.3. Effect of particle size

Fig. 5 shows the typical activation process of electrodes composed of different particle sizes. From Fig. 5 we see that the first discharge capacity increased with decreasing the particle size. But after 20 cycles, all the discharge capacities reached a saturation value. This indicates that the electrodes are fully activated and particle size has no significant effect on electrodes activation. However, the saturation values are higher for particles between 200–300 mesh and below 500 mesh. The capacity difference is about 15–20 mA h/g between the above particles and particles of 300–500 mesh. The reason for this may attributed to the difference of the contact resistance and charge transfer resistance among different particles. Naito et al. studied the charge transfer resistance and contact resistance for  $\text{MmNi}_{3.31}\text{Mn}_{0.37}\text{Al}_{0.28}\text{Co}_{0.4}$  electrode by using the impedance analysis method. One of their results

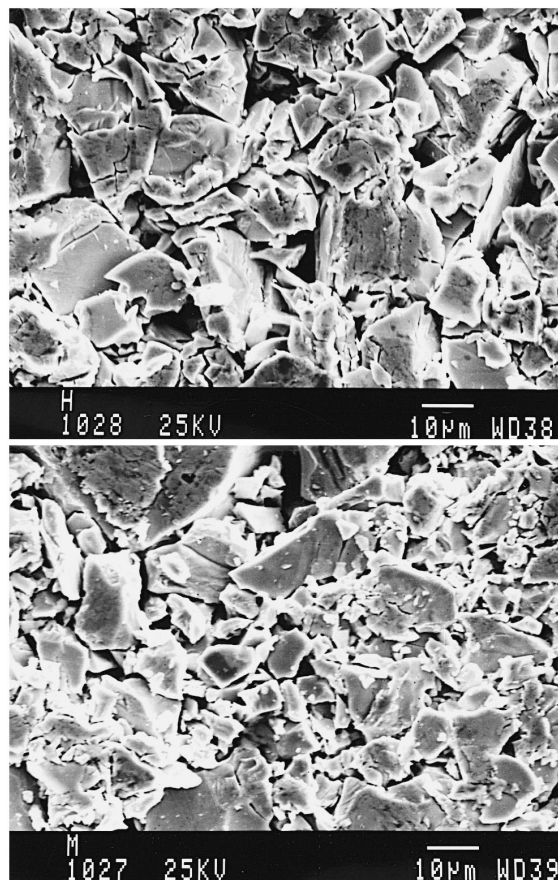


Fig. 4. (a) SEM image of alloy after hydrogen desorption pulverization. (b) SEM image of alloy after mechanical pulverisation.

indicated that both of the above resistances (contact and charge transfer) decreased with increasing particle size [12]. Therefore, the maximum discharge capacity should be obtained for particles between 200–300 mesh. This theory could not explain the higher discharge capacity for

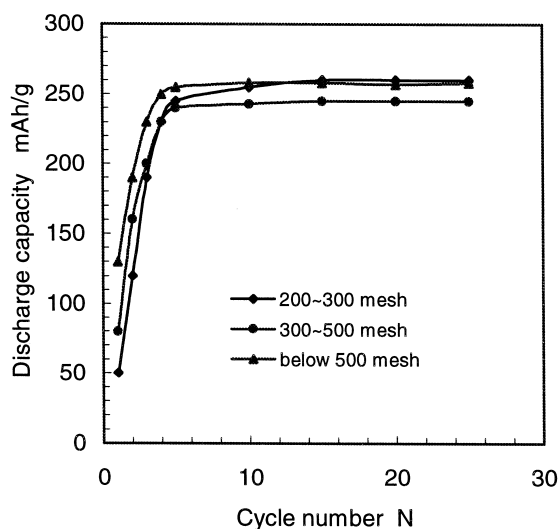


Fig. 5. Activation process of different particles.

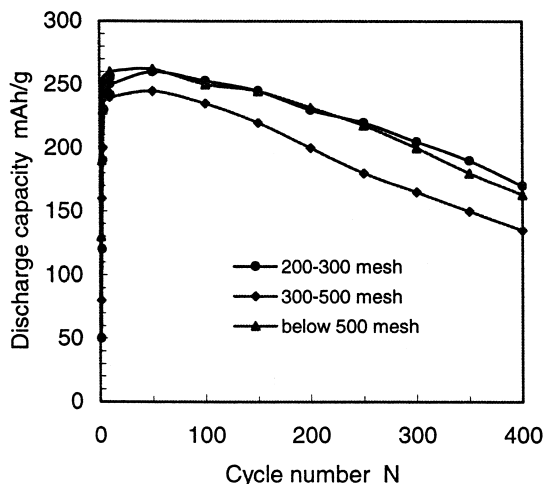


Fig. 6. Effect of particle sizes on the cycle life of electrodes.

particles below 500 mesh. Further analysing K. Naito's results (which are shown in their Table 1) suggested that both the charge transfer resistance and contact resistance changed with different forming pressure significantly for particles below 500 mesh. For example, for particles below 500 mesh. The contact resistance and charge-transfer resistance under the forming pressure of  $200/\text{kg cm}^{-3}$  were 0.16 and 1.06, respectively, but these two values dropped to 0.08 and 0.48 under a pressure of  $1200/\text{kg cm}^{-3}$ . While for the particles above 200 mesh, The contact resistance and charge-transfer resistance under the forming pressure of  $200/\text{kg cm}^{-3}$  were 0.09 and 0.58, respectively, but these two values only decreased to 0.07 and 0.42 under the pressure of  $1200/\text{kg cm}^{-3}$ . This suggests that particular particle size is correspondent with specific forming pressure for obtaining a lower contact and charge-transfer resistance. In other words, the forming pressure we employed may be more suitable for the particles under 500 mesh, which showed a higher discharge capability. Further experiments still need to be carried out to verify this.

Fig. 6 shows the capacity degradation with number of cycles for different particles. It could be seen that the capacity decay for particles of 200–300 mesh and below 500 mesh are less than that of particles between 300–500 mesh. The reason for this is not clear yet. One tentative explanation may be as following: suppose that the cycle life degradation mechanism was decided by effective hydrogen absorption materials during cycling. Because the larger particles have more effective materials than smaller ones during continuing cycles, it should be reasonable that the cycle life of larger particles is longer. But if the cycle life degradation mechanism was controlled by pulveriza-

tion due to discrete lattice expansion, the smaller particles may suppress pulverization of the alloys easily because the volume change induced by hydrogen absorbing/releasing is relatively small and is easier to relax. Therefore, the smaller particles may display better cycling performance under this condition.

#### 4. Conclusion

The effects of preparation on the characteristics of electrode have been investigated. Annealing made Co, Al and the rare earth elements more concentrated in the grain boundary and made La more concentrated in the grain, but homogenised the element Mn. The fluctuation of Mn may be the reason for the change of the p–c isotherm. Annealing decreased the capacity of electrode but improved the cycle life. Powder prepared by the hydrogen pulverization method displayed higher discharge capacity and rapidly activation characteristics. SEM micrographs indicated that the particles are more uniform and many small cracks could be observed in the grain after the hydrogen pulverization process. Investigation of the effect of different particle sizes on the properties of electrodes showed that the particles of 200–300 mesh and below 500 mesh have higher charge–discharge capability and a longer cycle life. This may due to the difference of the contact resistance and the charge-transfer resistance. Further study still needs to be carried out in order for practical application.

#### References

- [1] C. Witham, R.C. Bowman, *J. Electrochem. Soc.* 144 (1997) 3758–3764.
- [2] J.J. Willems, *Philips J. Res.* 39 (1984) 1, Suppl. 1.
- [3] F. Meli, A. Züttel, L. Schlapbach, *Z. Phys. Chem.* 183 (1994) 371.
- [4] T. Sakai, T. Hazama, H. Miyamura, N. Kuriyama, A. Kato, H. Ishikawa, *J. Less-Common Met.* 172–174 (1991) 1175–1184.
- [5] F. Meil, A. Züttel, L. Schlapbach, *J. Alloys Comp.* 231 (1995) 639–644.
- [6] P.H.L. Notten, J.L.C. Damms, R.E. Feinerhand, *Ber. Bunsenges Phys. Chem.* 96 (1992) 656.
- [7] G.D. Adzic, J.R. Johnson, J.J. Eeilly, J. Mcbreen, S. Mukerjee, *J. Electrochem. Soc.* 142 (1995) 3429–3433.
- [8] H. Nakamura, Y. Nakamura, S. Fujitani, Iyonezu, *J. Alloys Comp.* 218 (1995) 216–220.
- [9] H.M. Jin, Z.H. Wen, H.Y. Ren, G.X. Li, *Chin. J. Rare Earth* 21 (1997) 73–75.
- [10] D. Chartouni, F. Meli, A. Züttel, K. Gross, L. Schlapbach, *J. Alloys Comp.* 241 (1996) 160–166.
- [11] Y. Nakamura, K. Sato, S. Fujitani, K. Nishio, K. Oguro, I. Uehara, *J. Alloys Comp.* 267 (1998) 205.
- [12] K. Naito, T. Matsunami, K. Okuno, *J. Appl. Electrochem.* 23 (1993) 1051–1055.